11 Jun 2003

Catalytic Wet Oxidation of Phenol by Hydrogen Peroxide over Pillared Clay Catalyst

Jing Guo

Muthanna H. Al-Dahhan
Missouri University of Science and Technology, aldahhanm@mst.edu

Recommended Citation

J. Guo and M. H. Al-Dahhan, "Catalytic Wet Oxidation of Phenol by Hydrogen Peroxide over Pillared Clay Catalyst," *Industrial and Engineering Chemistry Research*, vol. 42, no. 12, pp. 2450 - 2460, American Chemical Society, Jun 2003.
The definitive version is available at https://doi.org/10.1021/ie020344t

Catalytic Wet Oxidation of Phenol by Hydrogen Peroxide over Pillared Clay Catalyst

Jing Guo and Muthanna Al-Dahhan*

Chemical Reaction Engineering Laboratory (CREL), Department of Chemical Engineering, Campus Box 1198, Washington University, St. Louis, Missouri 63130

Extrudates of Al−Fe pillared clay catalyst suitable for packed-bed operations are evaluated for wastewater treatment via a wet oxidation process employing hydrogen peroxide as the oxidant. The reaction was carried out in a semibatch basket reactor under rather mild conditions. Operational parameters were studied under the following conditions: temperature from 25 to 90 °C, atmospheric pressure, initial phenol concentration from 100 to 2000 ppm of the liquid phase, catalyst loading from 0 to 10 g/L, and input H_2O_2 concentration from 0.15 to 0.6 mol/L. Under these conditions, the Al−Fe pillared clay catalyst achieves a total elimination of phenol and significant total organic carbon (TOC) removal. This catalyst can be used several times without any change in its catalytic properties, and hence, it would be a promising catalyst for industrial wastewater treatment. The reaction takes place to a significant extent both in the liquid phase and on the catalyst surface. Hence, apparent kinetic models were developed by formulating the reaction rate in two kinetic expressions that separately consider the homogeneous and heterogeneous contributions. Using the second-order approach for the homogeneous reaction and the Langmuir−Hinshelwood approach for the heterogeneous reaction, the developed kinetic models describe well the removal of phenol and the formed intermediate carbon over the entire range of the variables studied.

Introduction

Industrial processes and agricultural activities generate a large diversity of wastewater containing organic pollutants. Such wastewater has become a major social and economic problem, as modern health-quality standards and environmental regulations have gradually become more restrictive.[1] Phenol and phenolic substances are used as raw materials in many petrochemical, chemical, and pharmaceutical industries. In the past 2 decades, however, wastewater containing phenol has received increased attention because of its toxicity and prevalence in industrial processes.[2,3] In addition, phenol is considered to be an intermediate product in the oxidation pathway of higher-molecular-weight aromatic hydrocarbons.[4] Thus, it is usually taken as a model compound for advanced wastewater treatment studies.

In selecting a wastewater treatment process among chemical, biological, and catalytic methods, one should take into account the toxicities and concentrations of the pollutants in the waste stream. The pollutants' concentrations should be high for chemical destruction methods that are thermally self-sufficient, whereas bioprocesses are suitable for nontoxic pollutants at low concentrations.

Biological treatment usually involves the activity of microorganisms, which oxidize and convert the organic matter to CO_2. Anaerobic sewage treatment involves a complex series of digestive and fermentative reactions carried out by a host of different bacterial species, whereas aerobic treatment allows wastewater to be treated via the trickling filter or activated sludge. Both processes can treat huge amounts of wastewater at one time.[5] However, it is known that routine biological methods are not effective for the wastewater generated by the chemical, agricultural, and pulp and paper industries, which contains organic pollutants in the range of a few hundred to a few thousand parts per million. These wastes are too dilute to incinerate, yet too toxic to be biologically treated.[6] Examples of toxic and hence nonbiodegradable organic pollutants are phenols, surfactants, chlorinated compounds, pesticides, aryl- and chlorinated alkylsulfonates, polyethylene, and aromatic hydrocarbons.[7] In addition, biodegradation processes are inherently slow, and they do not allow for high degrees of removal.[4] The disposal of sludge formed during biological treatment can pose additional expenses and environmental problems. Evidently, the biological treatment of industrial wastewater is of limited use only, and additional treatment by other methods is frequently required.[1] Because biotreatment is ideally suited for low concentrations, typically around 50 ppm or lower for phenol,[8] diluting wastewater to a suitable concentration for the microorganisms leads to economically unfeasible volumes.

One more promising process for aqueous waste treatment is catalytic wet oxidation (CWO), which uses oxygen (air), ozone, hydrogen peroxide, or a combination as the oxidative agent. CWO destroys a variety of organics released in wastewater effluents with the addition of a catalyst, achieving a high conversion of the organic pollutants. Hence, the biological methods could serve as a complementary application for CWO.

Such recourse to solid catalysts offers a practical technological alternative to the conventional noncatalytic or homogeneously catalyzed routes. Not only can the treatment tolerate milder conditions (temperature and pressure), but, in principle, the catalyst can also be easily recovered, regenerated, and reused. Another

* Corresponding author. Telephone: (314) 935-7187. Fax: (314) 935-7211. E-mail: muthanna@che.wustl.edu.

10.1021/ie020344t CCC: $25.00
Published on Web 02/21/2003

considerable advantage of catalytic methods is the possibility of treating only a single pollutant, or a group of similar pollutants, out of complex mixtures of pollutants (as in selective catalytic reduction).[9] This opportunity is of special interest when a mixture of pollutants and useful compounds must be processed. By proper choice of the catalyst, it is possible not only to control the degree of conversion of pollutants but also to select different reaction routes, thereby selecting the optimal reaction intermediates and products and avoiding the formation of secondary pollutants.[10] As an alternate method for purifying wastewaters, CWO involving solid catalyst has been successfully applied to wastewaters discharged from petroleum and petrochemical industries that are contaminated with toxic or refractory substances inappropriate for biological treatment.[11]

The typical features of industrial operation of CWO are high temperature (200−325 °C) and high pressure (5−15 MPa, higher than the vapor pressure of water at these temperatures). Further improvement of catalyst performance, however, is needed for wider use of the wet oxidation process. If a catalyst can be developed that works effectively below 150 °C, catalytic wet oxidation would be a potential process for more general water treatment.[9]

A diversity of solids have been used as catalysts for the oxidation of various organic compounds in wastewater.[12] To reduce the severity of the operating conditions, several newly developed catalysts have been proposed, such as MnO_2/CeO_2 and Pt-promoted MnO_2/CeO_2.[13] Although wet oxidation of phenol over composite oxide was remarkably fast at mild temperature (80−130 °C) and pressure (0.5−2.5 MPa O_2) conditions, the catalyst underwent severe deactivation. This deactivation was found to be induced by the formation of carbonaceous deposits on the catalyst surface, which irreversibly adsorbed on its active sites.[14] The catalyst's poor selectivity to CO_2 was also demonstrated to result from deposition of carbon on the catalyst surface. Promotion of MnO_2/CeO_2 with platinum improved the CO_2 yield of phenol oxidation. However, platinum-promoted MnO_2/CeO_2 was more sensitive to deactivation and exhibited systematically lower degradation rates of phenol and total organic carbon.[13]

Pillared clay represents a new class of microporous materials that have potential for use as catalysts. A great deal of progress has been made in understanding these materials, particularly their catalytic behavior.[15] The impetus behind the original work was to create three-dimensional porous structures from two-dimensional clay minerals. It was expected that pores larger than those available in zeolites would be obtained.[15] Recently, by using powdered catalyst and hydrogen peroxide as the oxidant, clay-based catalysts pillared by mixed Al−Fe complexes have shown encouraging results for oxidizing aqueous organic compounds in a slurry laboratory-scale reactor. Under mild experimental conditions (atmospheric pressure, $T < 70$ °C) and low excess (20%, mole) of hydrogen peroxide, 80% of the initial amount of phenol was converted mainly to CO_2 within 4 h. The Al−Fe pillared clay catalyst can be used several times without significant catalyst leaching and deactivation.[16]

Using a reactor modeling framework for CWO, Larachi et al.[6] comparatively analyzed the performance of different reactor configurations, such as packed-bed, three-phase fluidized bed, and slurry bubble column. The simulation results showed that packed-bed reactors outperformed fluidized beds and slurry bubble columns for the CWO process. Thus, newly developed extrudates of Al−Fe pillared clay catalyst suitable for packed-bed operations have been manufactured for further investigation utilizing different oxidants (e.g., peroxide only, air only, peroxide plus air). Before the performance of this catalyst can be evaluated in packed-bed reactors, the apparent kinetics and the catalyst performance need to be studied in a stirred-basket reactor for the purpose of reactor modeling and process optimization. The present work is intended to focus on the study of the decomposition of aqueous phenol by using only hydrogen peroxide over mixed Al−Fe pillared clay catalyst.

Experimental Work

Materials. Phenol (Ph, >99.5% purity) was purchased from Sigma-Aldrich Corporation. Hydrogen peroxide (30% in water, ACS reagent grade) was supplied by Eastman Kodak Company. Analytical-grade hydroquinone, benzoquinone, oxalic acid, acetic acid, and catechol used to identify the reaction intermediate were also supplied by Sigma-Aldrich Corporation.

Catalyst Characterization. Al−Fe pillared clay catalyst particles in cylindrical form (2 × 8 mm, approximately) were supplied by Professor N. Papayannakos' process analysis and plant design group, National Technical University of Athens (NTUA), Athens, Greece. They had been prepared by extruding a pillared Greek bentonite called Zenith-N. NaOH solution was slowly added to the Al^{3+}/Fe^{3+} cationic solution (i.e., the solution containing the positively charged ion) at 70 °C until the OH/cation mole ratio was equal to 1.9. The intercalant solution was added to the clay suspension under stirring. The final (Al + Fe)/clay ratio was equal to 3.8 mol/kg of dry clay. After being aged for 24 h, the pillared clay precursor was washed until total elimination of chloride ions, dried at 60−70 °C, and finally calcined at 500 °C for 2 h. The main composition (wt %) was as follows: SiO_2, 52.50; Al_2O_3, 27.56; Fe_2O_3, 7.02.[16]

The pore diameter, specific surface area, and pore volume of the pillared clay catalyst extrudates were determined as 1.80 ± 0.02 nm, 180 m^2/g, and 0.33 cm^3/g, respectively.

Apparatus, Procedure, and Analysis. Experimental investigations were carried out in a stainless steel autoclave basket reactor. In batch operation, the liquid phase was 600 mL of aqueous solution of phenol. Hydrogen peroxide was continuously fed to the reactor at flow rates ranging from 0.21 to 0.84 mol/min. This low rate of hydrogen peroxide addition was chosen to minimize its consumption and to maximize the efficiency of its use. The reactor was heated to the reaction temperature, which was measured and controlled in the liquid phase, with its value held constant to within ±0.5 °C. When the temperature became steady, hydrogen peroxide was fed into the reactor by a Milton Roy pump at constant flow rate. This point was taken as the "zero time" for the experimental records. Experimental runs were carried out at different temperatures (from ambient temperature to 90 °C), and different catalyst loadings ($C_{cat} = 0-10$ g/L), different initial phenol concentrations (100−2000 ppm). Liquid samples were taken from the reactor at preset time intervals so that sample concentration, total organic carbon (TOC), and pH could be measured. The reactor was equipped with a six-blade

turbine-type impeller mixer, with the rotation speed being increased until the external mass-transfer resistance was minimized.

The phenol conversion and product distribution were analyzed by high-performance liquid chromatography (HPLC) with a system consisting of a Waters 510 HPLC pump, a Micromeritics 725 autoinjector, and an LDC/Milton Roy SpectroMonitor 3000 as the detector. UV detection was employed at $\lambda = 211$ nm. The column contained Waters Spherisorb 5-μm ODS2 (4.6 × 250 mm) as the stationary phase and a mixture of 35/65 (methanol/water, v/v, HPLC grade) as the mobile phase. The flow rate of the mobile phase was set to be 1 mL/min. Total organic carbon (TOC) was detected by a Shimadzu TOC-500 analyzer. The value of the pH in fresh and reacted solution was measured by a model IQ240 pH meter from Scientific Instruments Inc.

Results and Discussion

Intermediate Products Identification. By using the HPLC setup, the retention time of a single compound was identified by injecting pure samples of the expected partial oxidation products. Then, by using aqueous samples of known composition, calibration curves were developed for each detected intermediate product. The main detected intermediates in the product effluent were acetic acid, catechol, and hydroquinone. Oxalic acid and benzoquinone were also identified in measurable quantities. However, malonic and formic acids were detected only as traces, below 10 ppm. No other compounds were detected in measurable amounts. No condensation products were found in the exiting solution or deposited on the catalysts.

Quinone-like products such as hydroquinone, benzoquinone, and catechol were identified in the first stages of the phenol oxidation pathway. These byproducts need to be removed because they are as toxic as phenol. Figure 1a shows the profiles of quinone-like products, where the existence of maximum points for hydroquinone, benzoquinone, and catechol were demonstrated. These profiles exhibit a common characteristic of the consecutive reaction pathway in which quinone-like products are formed from more complex intermediates and degraded progressively to simpler organic compounds.[17] Benzoquinone itself could lead to the observed color change of the reacting solution, whereas fresh phenol solution is colorless. With increasing reaction time, the color of the solution gradually changed from light to dark brown and then back to light brown. After 4 h, the solution became almost colorless. The dark brown color is due to the formation of benzoquinone during phenol oxidation. With further oxidation, benzoquinone is mineralized or degraded to low-molecular-weight organic acids, leading to a colorless solution.

For all of the figures presented, each experimental data point is the mean value resulting from triplicate analysis of the corresponding sample. The reproducibility lies within the data point's area. Hence, error bars are not shown in all of the figures. Figure 1b shows the oxalic acid and acetic acid concentrations against the reaction time. Unlike quinone-like products, the profiles do not have a maximum, which indicates that these low-molecular-weight acids can be taken as the end products of the complex phenol oxidation network. This behavior is due to the resistance of low-molecular-weight carboxylic acids, acetic acid in particular, to catalytic wet oxidation, which is a major limitation of the CWO technology.[18] However, the carboxylic acids could easily be eliminated by the biological step of β oxidation.[5] Therefore, this process could be used as a chemical pretreatment step for wastewater containing high phenol concentrations harmful to a biological treatment system.

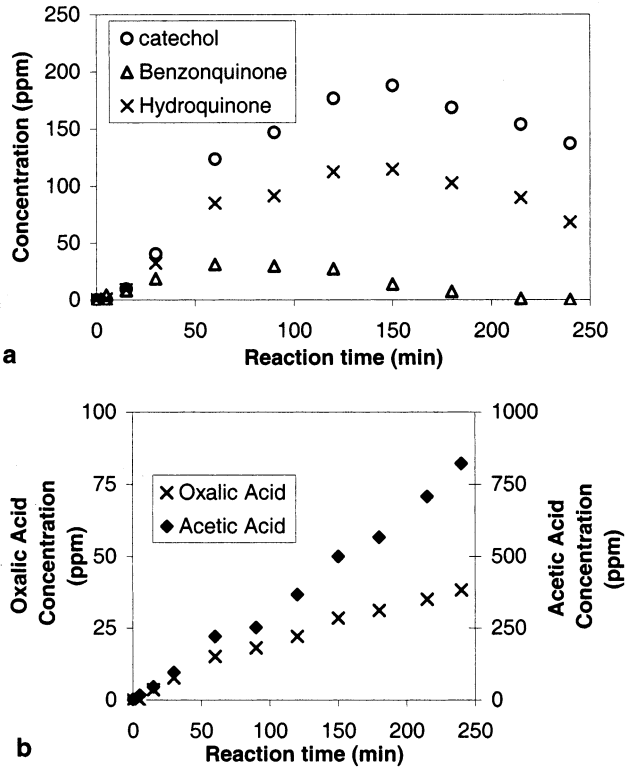

Figure 1. Evolution of intermediate product concentrations (70 °C, 1 g/L phenol, 6.6 g/L catalyst, 0.3 mol/L H_2O_2, initial pH = 3.9).

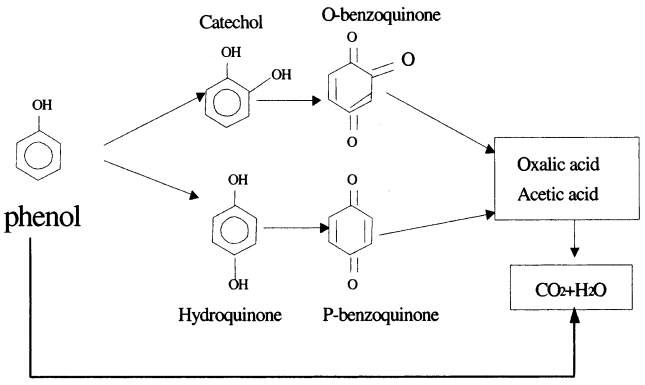

Figure 2. Proposed reaction scheme for the phenol oxidation.

Figure 2 presents the simplified reaction scheme for the oxidation of phenol, where the important interconnection between the presence of quinones and organic acids can be seen. The first step represents the formation of intermediate ring compounds, namely catechol, hydroquinone, and benzoquinones, whereas the subsequent stage corresponds to the cleavage of intermediates and the formation of carboxylic acids. This scheme is in line with the conclusion of Fortuny et al.,[19] except that the possibility of direct decomposition of phenol to inorganic carbon during the ring-opening reaction is also taken into account in this study, as was also mentioned by Ding et al.[20]

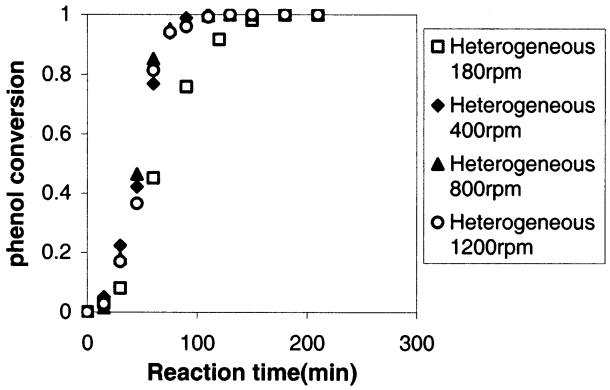

Figure 3. Effect of rotation speed (rpm) on catalytic phenol conversion (70 °C, 500 ppm phenol, 0.6 M H_2O_2, 6.6 g/L catalyst).

Effect of Impeller Rotation Speed. To observe the apparent reaction rate of phenol oxidation, the external mass-transfer resistance for the species to transfer to the surface of the catalyst must be minimized. Hence, the effect of the impeller rotation speed was investigated to identify the rate (in rotations per minute, rpm) above which the apparent reaction rate would not change. The rotation speed was varied from 180 to 1200 rpm while other conditions were maintained at 70 °C, 500 ppm phenol, and 6.6 g/L catalyst loading. Figure 3 shows that the conversions with time are independent of rotation speed above 400 rpm. Therefore, to neglect the external mass-transfer resistances in the following experiments, the rotation speed was kept at 800 rpm.

Effect of the Initial Solution pH. The mechanism of wet oxidation using H_2O_2 could be considered as a radical reaction with $OH^{\bullet}$, $HO_2^{\bullet}$, or $ROO^{\bullet}$ radicals being the main oxidants.[21] The stability of hydrogen peroxide is dependent on pH. The least decomposition of H_2O_2 was found at pH values between 3 and 4.[22] This range corresponds to the highest stability zone of $[Fe(OH)]^{+2}$. Above pH 4, the rapid hydrogen peroxide decomposition rate produces molecular oxygen without formation of appreciable amounts of available hydroxyl radicals in the solution. Below pH 3, more of the charged ferric ions remained as hydrated ferric ions, which accelerate not only the decomposition of the peroxide but also the competitive reaction for hydroxyl radicals depletion.[21] In addition, pH lower than 3 favors leaching of the metal into the solution.

Phenol is a relatively weak acid that confers slight acidic properties to the aqueous solution. Without pH adjustment, the initial solution of phenol and deionized water exhibited pH value between 5.8 and 6.0 in the current experiments. At this pH range, phenol conversion curves show a sigmoidal profile, as seen in Figure 4, which is typical of autocatalytic or radical reactions. There are two different regions, one for the initial part of the curve, which represents the induction period, and the other for the part after the inflection point, which represents the steady state. It is well-established in phenol chemistry that the optimum pH for the maximum reaction rate is about 4.0 for both the induction period and the steady-state regime.[21]

To test the effect of pH, hydrochloric acid was added into the solution to adjust the initial pH value to 3.9−4.0. Figure 4 shows the phenol removal results for two initial phenol concentrations with respect to time at two initial values of solution pH. The initial rate of oxidation is markedly affected by pH, whereas the steady-state

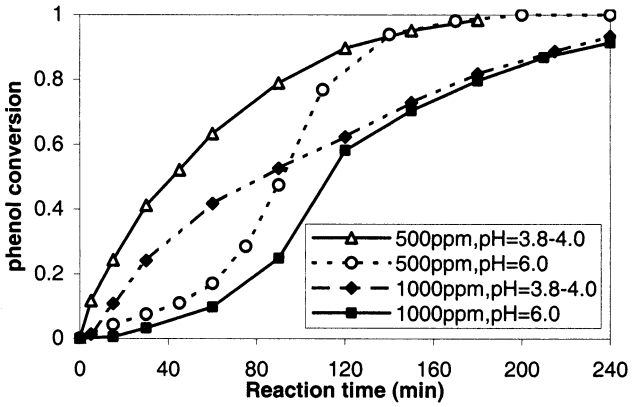

Figure 4. Effect of initial solution pH on catalytic phenol conversion (70 °C, 0.3 M H_2O_2, 6.6 g/L catalyst).

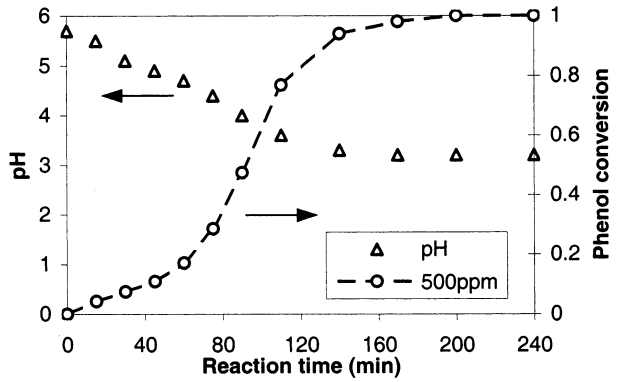

Figure 5. Evolution of pH value and phenol conversion for solution without the addition of acid (70 °C, 0.3 M H_2O_2, 6.6 g/L catalyst).

activity is a much weaker function of the pH. For either 500 or 1000 ppm phenol solution, there is a significant difference in the induction period of oxidation between the solution with and without pH adjustment: the time required to reach the steady state decreases as the pH decreases. However, when the steady state is reached, the phenol conversion curves fall almost into the same line. It is evident that a solution with adjusted pH gives better results in terms of the reaction rate for the whole process, where the various radicals or intermediates in the chain-propagation reactions are rapidly formed and reacted. Thus, the steady state could be quickly reached during the operation, and the inflection point could be circumvented. Consequently, all of the following experiments were based on an initial solution pH of 3.9−4.0. However, it is worth noting that the choice of HCl to adjust the pH of the solution is not the best one because of the concern over HCl evaporation at high temperature. Although no significant HCl evaporation was observed in this work at the studied mild temperature, it is recommended that H_2SO_4 be used for further experiments under higher-temperature conditions.

The reaction intermediates from the complex phenol oxidation mechanism give rise to organic acid, which enhances the acidity of the reaction solution even more. Interestingly, even without pH adjustment, the batch solution pH could still reach around 3.5, as shown in Figure 5. Hence, for practical industrial operation, the effluent solution itself could be recycled and used to adjust the initial pH value, which means additional usage of acid could be avoided.

Effect of Temperature. Increasing the reaction

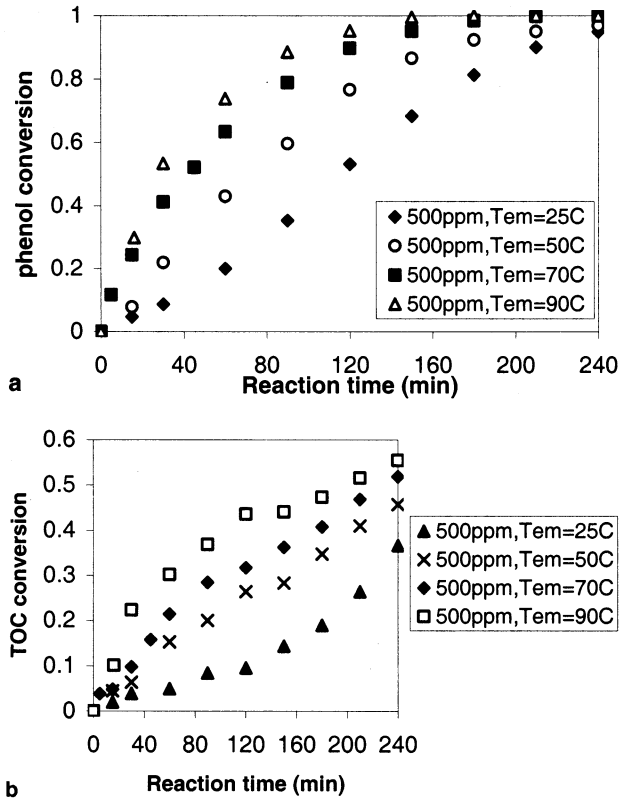

Figure 6. Effect of temperature on (a) phenol and (b) TOC removal by catalytic oxidation (500 ppm phenol, 6.6 g/L catalyst, 0.3 M H_2O_2).

temperature leads to two opposite effects. The phenol oxidation rate increases according to the Arrhenius equation, but the destruction rate of H_2O_2 to O_2 and H_2O also increases at high temperature. Therefore, it is necessary to optimize these two effects by controlling the temperature.

Total organic carbon (TOC) analysis is used to characterize intermediate residues and the degree of organic carbon mineralization in the liquid phase. Figure 6a and 6b presents the changes in phenol and TOC, respectively, under different temperatures in the range of 25−90 °C. The continuously added amount of H_2O_2 could eliminate 500 ppm of phenol in the aqueous solution after 175 min at 90 °C. Even at ambient temperature (25 °C), the catalytic oxidation process still could remove phenol completely in approximately 300 min. Higher phenol and TOC removal rates were observed at higher temperatures. The effect on the phenol removal rate of increasing the temperature from 70 to 90 °C is not as significant as the effect of increasing the temperature from 50 to 70 °C, because of the higher decomposition rate of H_2O_2 at higher temperature. The capability of the catalyst to destroy phenol at low temperature highlights this catalyst's promising industrial application.

The TOC removal rate is less than the phenol elimination rate, showing clearly that phenol oxidation takes place in multiple steps and results in several byproducts rather than CO_2 only. In addition, the TOC removal is also noticeably affected by reaction temperature. It is obvious that the removal of phenol occurs much more quickly than the degradation of short-chain organic acid, which is formed from the phenol oxidation and is stable and refractory to further oxidation into CO_2 and H_2O in CWO.

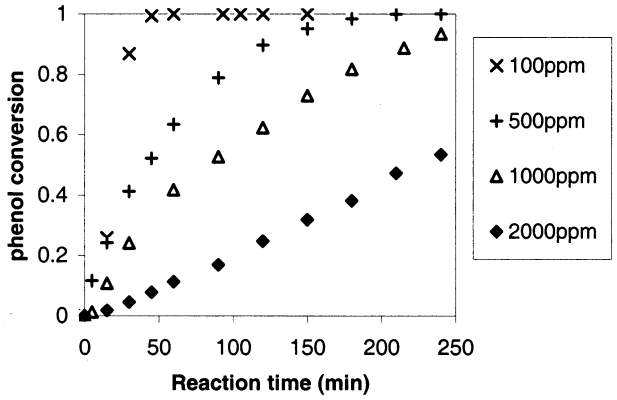

Figure 7. Effect of initial phenol concentration on phenol reduction by catalytic oxidation (70 °C, 0.3 M H_2O_2, 6.6 g/L catalyst).

Effect of Phenol Concentration. The effect of the initial concentration of phenol was investigated in the range of 100−2000 ppm at 70 °C in the presence of catalyst. Figure 7 shows the phenol conversion with time at four initial phenol concentrations, which demonstrates that a higher initial phenol concentration leads to lower conversion under otherwise identical conditions. The same self-inhibiting effect of the phenol initial concentration on the oxidation rate was observed by Pintar and Levec.[23] Stoichiometrically, the continuous flow of hydrogen peroxide could mineralize 100 and 500 ppm of aqueous phenol after 75 and 375 min, respectively. Experimental data indicate that it took within 50 and 210 min to totally destroy the phenol with initial concentrations of 100 and 500 ppm, respectively. The time required for phenol removal is less than that needed for phenol mineralization, which shows the existence of a multipathway reaction.

In addition, it takes much longer to remove phenol when the solution is more concentrated, such as 1000 and 2000 ppm aqueous solutions. Thus, CWO could perform better for low concentrations of aqueous phenol.

Effect of H_2O_2 Concentration. Figure 8a shows the time dependence of phenol conversion at four H_2O_2 concentrations, corresponding to about 25, 50, 100, and 600% of the stoichiometric amount required for complete removal of aqueous phenol at 180 min. The reaction temperature was maintained at 70 °C so that the oxidation reaction rate would be pronounced and the decomposition rate of H_2O_2 could be neglected. A higher initial rate of phenol removal results from a higher H_2O_2 concentration, which means that the H_2O_2 concentration needs to be considered in the kinetics expression. However, when O_2 is used as the oxidative agent, the O_2 term is seldom included in the kinetics expressions in the literature because of the negligible influence of the O_2 pressure.

The intermediate carbon profiles, shown in Figure 8b, display clearly that a higher H_2O_2 concentration allowed the intermediate product concentrations to reach a maximum within a shorter period. With 0.6 M H_2O_2 continuously added into the reactor, the intermediate carbon reached a maximum at 50 min, and 35% of the carbon was mineralized from phenol oxidation according to the carbon balance. The intermediate carbon was then consumed by H_2O_2, and the removal of intermediate carbon reached a plateau after 180 min. At that time, 100% of the stoichiometric amount of H_2O_2 was attained, and 93% of the original carbon was mineralized. A further increase in H_2O_2 did not result in more

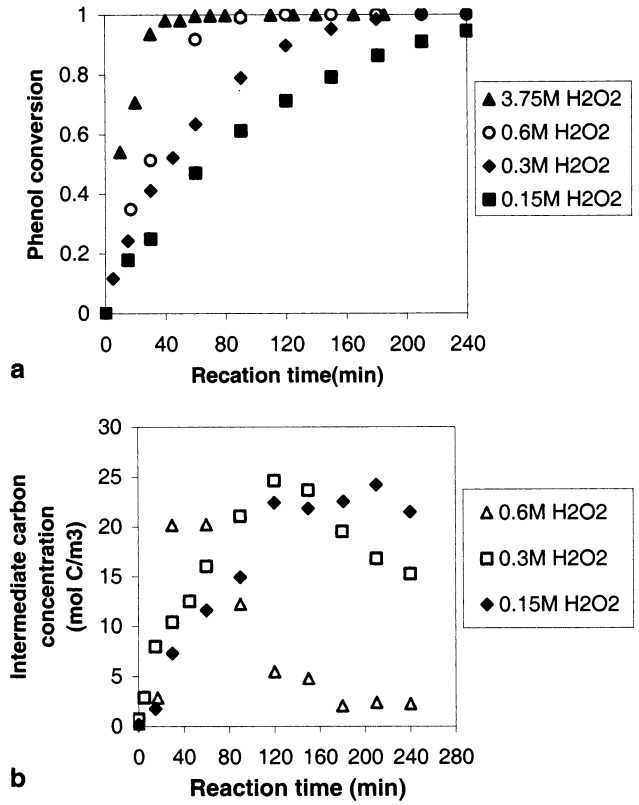

Figure 8. Effect of H_2O_2 concentration on (a) phenol conversion and (b) intermediate carbon during CWO (70 °C, 500 ppm phenol, 6.6 g/L catalyst).

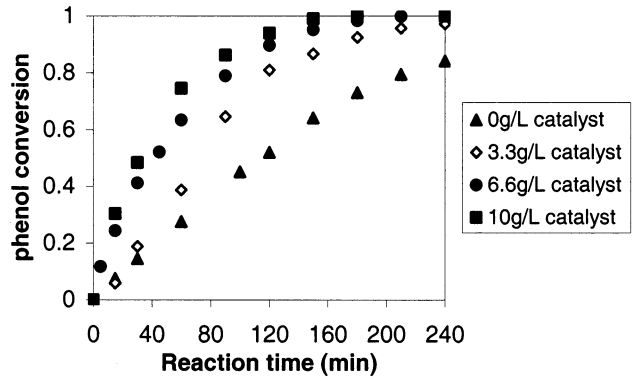

Figure 9. Effect of catalyst loading on phenol oxidation (70 °C, 500 ppm phenol, 0.3 M H_2O_2).

profile change. Thus, the pathway of intermediate carbon suggests that the oxidation process involves the mineralization and breakdown of phenol to daughter organic intermediates at the same time, which confirms the reaction scheme shown in Figure 2. The breakdown reaction leads to the formation of high-molecular-weight intermediates and then further degradation into low-molecular-weight acid. The residual intermediates as mainly organic acids are refractory to mineralization.

Effect of Catalyst Loading. The effect of catalyst loading was investigated at 70 °C and an initial phenol concentration of 500 ppm. The homogeneous reaction in the absence of catalyst is pronounced. Still, as Figure 9 shows, the presence of the catalyst significantly enhances the oxidation rate of phenol. In addition, it is clearly demonstrated that an increase in catalyst concentration considerably improves the rate of phenol degradation. The involvement of a heterogeneous−homogeneous mechanism in the induction period is indicated by the observed dependence of the initial rate on the catalyst concentration.

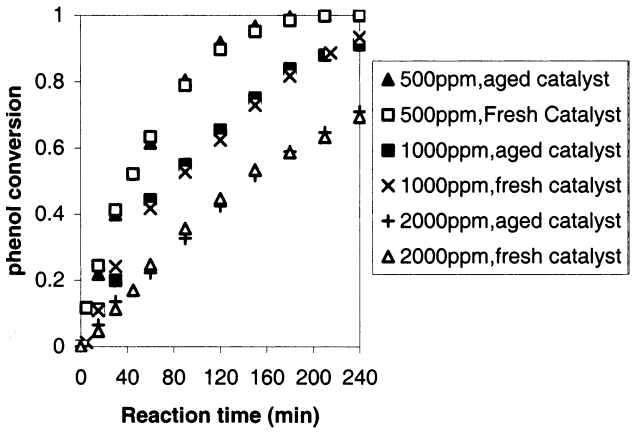

Figure 10. Comparison of catalyst performance between the fresh catalyst and the aged catalyst (70 °C, 0.3 M H_2O_2, 6.6 g/L catalyst).

Recycling of the Catalyst. Additional oxidation tests were carried out by contacting fresh phenol solutions with aged catalyst taken from previous runs, so that the capability of aged pillared clay catalyst to destroy phenol could be evaluated. As shown in Figure 10, the oxidation of 500, 1000, and 2000 ppm phenol at 70 °C over aged catalyst did not indicate any significant difference compared to oxidation over the fresh catalyst. It is obvious that the catalyst deactivation during these reactions could be negligible.

Even though the reaction solution was acidic (pH = 3−4) and the slurry catalyst was used, the contribution of iron ions leached from the clay can be positively considered insignificant as less than 0.4 ppm of iron was measured in the reaction solution after 4 h of experiment. In addition, the cumulative elution of Al−Fe iron in three experiments was found to be less than 0.2% of the total iron content in this catalyst.[16] The low iron leaching shows that there exists a strong interaction between iron and aluminum pillars. About 60% of the iron species is bonded to the small oxide clusters dispersed in the solid, inside or outside the porosity. Regardless of the location, the iron species are highly stabilized by the clay matrix.[24] Our work deals with the extruded catalyst particle in cylindrical form, which would result in even less metal leaching compared to that from slurry catalyst. The low leaching and high catalytic activity show that this catalyst could be a promising catalyst for industrial wastewater treatment.

Apparent Kinetics Model Development

For the catalytic oxidation of aqueous phenol or similar organic pollutants, the kinetic models proposed in the literature are in terms of either power laws[21] or more complex equations based on adsorption−desorption mechanisms, i.e., Langmuir−Hinshelwood−Hougen−Watson (LHHW) models.[17] Most of the CWO studies utilized pure O_2 or air as the oxidant and concluded that no significant effect of the homogeneous reaction exists.[14] However, in an investigation of the catalytic oxidation of 4-chlorguaiacol, it was found experimentally that the homogeneous reaction was significant that the kinetics study should not neglect it. Thus, by assuming that the homogeneous and heterogeneous reaction rates are additive, a compre-

hensive network model was suggested to account for the significant reaction both in the liquid bulk phase and on the catalytic surface by combining a two-parallel-reaction scheme for the noncatalytic oxidation and a Langmuir−Hinshelwood approach for the catalyst-mediated oxidation.[25]

In the current work on phenol oxidation with hydrogen peroxide as the oxidant, experimental evidence indicates that approximately 30−40% of hydrogen peroxide homogeneously decomposes in the liquid bulk, while the other portion decomposes in contact with the clay catalyst. Because both noncatalytic and catalytic oxidation occur simultaneously, the method proposed by Hamoudi et al.[25] could be utilized to study the roles of the catalyst in the homogeneous (noncatalytic) and heterogeneous (catalytic) reactions separately.

To account for the effect of catalyst loading on the CWO reaction rate, some literature papers assume a linear dependence of the reaction rate on the catalyst.[25] In other papers the influence of catalyst loading is expressed in terms of an empirical correlation.[4] To consider rigorously the influence of catalyst loading on the catalyst-mediated reaction, a complex radical mechanism should be developed, which is beyond the scope of this study. Therefore, in this study, the catalyst loading term in the heterogeneous reaction rate is modified in an empirical way by including the exponent terms for both the phenol removal and the intermediate product degradation. To preserve the units of the reaction rates, it has been shown that the exponent terms have to have the same value p, as shown in eq 1

$$-\frac{d[A]}{dt} = r_{h,A} + r_{H,A}C_{cat}{}^{p}$$

$$\frac{d[B]}{dt} = r_{h,B} + r_{H,B}C_{cat}{}^{p} \qquad (1)$$

where the initial conditions are $[A] = [A]_0$ and $[B] = 0$.

The experimental data and findings, discussed earlier for phenol removal and intermediate product degradation during homogeneous (without catalyst) and heterogeneous (with catalyst) wet oxidation, are utilized to obtain the mathematical description of this complex reaction network, as shown in Figure 2. Three basic lumps are considered in the reaction system, which are expressed in carbon concentration terms for oxidation kinetics: (1) phenol, denoted as lump A, is the parent pollutant to be removed; (2) intermediate organic carbon, denoted as lump B, is the phenol oxidation byproduct; and (3) total inorganic carbon, denoted as lump C, is the fully mineralized end products.

On the basis of the carbon scale, $[B] = TOC - [A]$ and $[C] = [A]_0 - TOC$, which could be determined using HPLC and TOC analysis. Accordingly, the development of the apparent kinetics models involves the following steps: (1) development of the homogeneous kinetics model (with rate r_h) using the homogeneous experimental data, and (2) development of the heterogeneous kinetics model (with rate r_H) using the heterogeneous experimental data and the developed homogeneous model with its fitted parameters.

Homogeneous Kinetics Model. To model the homogeneous contribution, i.e., the noncatalytic oxidation route with rate r_h, a sequential−parallel reaction scheme is proposed where the production of lump C is generated by irreversible oxidation of both lump A and lump B. Lump B results from the irreversible oxidation of lump A. The elementary steps are shown in eqs 2, which is consistent with the proposed reaction pathway of phenol oxidation shown in Figure 2.

$$H_2O_2 + A \xrightarrow{k_{h,1}} B$$

$$H_2O_2 + A \xrightarrow{k_{h,2}} C \qquad (2)$$

$$H_2O_2 + B \xrightarrow{k_{h,3}} C$$

Similar elementary steps were proposed by Li et al.[26] for the generalized wet oxidation of organics with O_2 from air as the oxidant, where the apparent reaction kinetics is first-order with respect to the organic reactant and zero-order with respect to O_2, if the oxygen partial pressure and gas−liquid mixing are sufficient. In this study, because the experimental data show that not only organic reactants but also H_2O_2 have effects on the oxidation reaction rate, the reaction kinetics could be taken as first-order in both organic reactant and H_2O_2.

The reaction rates with respect to lumps A and B are given in eqs 3. According to the experimental data, the following coupled ordinary differential equations are solved to obtain the time dependence of the concentrations of species A and B

$$-\frac{d[A]}{dt} = r_{h,A} = (k_{h,1} + k_{h,2})[A][H_2O_2]$$

$$\frac{d[B]}{dt} = r_{h,B} = k_{h,1}[A][H_2O_2] - k_{h,3}[B][H_2O_2] \qquad (3)$$

with the initial conditions $[A] = [A]_0$ and $[B] = 0$ at $t = 0$.

Examining the mass balance of H_2O_2 leads to the following expression for the concentration of H_2O_2

$$\frac{d[H_2O_2]}{dt} = \frac{u[H_2O_2]_{in}}{V} - r_{H_2O_2} \qquad (4)$$

where $r_{H_2O_2} = (k_{h,1} + k_{h,2})[A][H_2O_2] + k_{h,3}[H_2O_2][B]$, which represents the depletion rate of H_2O_2 with the initial condition $[H_2O_2] = 0$ at $t = 0$.

Heterogeneous Apparent Kinetics Model. In the presence of catalyst, both the heterogeneous and the homogeneous oxidation reactions take place at the same time. Once the homogeneous oxidation kinetics parameters are established and known, the parameters for the heterogeneous oxidation model are obtained by combining the heterogeneous experimental data with the fitted homogeneous reaction kinetic parameters.

The heterogeneous elementary steps are characterized by adsorption of the reactants on the active sites of the catalyst (represented by *), followed by surface reaction and desorption of the products back into the liquid, which can be presented as follows

$$A + * \xleftrightarrow{K_{H,A}} A*$$

$$H_2O_2 + A* \xrightarrow{k_{H,1}} B*$$

$$H_2O_2 + B^* \xrightarrow{k_{H,2}} C + *$$

$$B^* \xleftrightarrow{K_{H,B}} B + * \quad (5)$$

Hydrogen peroxide is assumed to remain unadsorbed on the active sites and to react directly with chemisorbed phenol. In addition, the steps of adsorption and desorption are assumed to be instantaneous as compared to surface reactions of chemisorbed phenol and its daughter intermediate products, which are the rate-controlling steps. To describe the catalytic reaction between phenol and O_2, Pintar and Levec[17] reported the similar LHMW approach that is complicated but useful for the prediction of reaction mechanisms based on elementary reaction rate constants. In this case, with H_2O_2 as the oxidant, the depletion rates of phenol and intermediate product due to the heterogeneous reaction can be described by the following equations

$$r_{H,A} = \frac{k_{H,1}K_{H,A}[A][H_2O_2]}{1 + K_{H,A}[A] + K_{H,B}[B]}$$

$$r_{H,B} = \frac{k_{H,1}K_{H,A}[A][H_2O_2]}{1 + K_{H,A}[A] + K_{H,B}[B]} - \frac{k_{H,2}K_{H,B}[B][H_2O_2]}{1 + K_{H,A}[A] + K_{H,B}[B]} \quad (6)$$

Now, the final model equations for the catalytic oxidation are obtained by substituting eqs 3 and 6 into eq 1, which leads to the overall reaction rate expressions for the phenol and intermediate products with the presence of catalyst given in eqs 7

$$-\frac{d[A]}{dt} = r_{h,A} + r_{H,A}C_{cat}{}^p = (k_{h,1} + k_{h,2})[A][H_2O_2] + \left[\frac{k_{H,1}K_{H,A}[A][H_2O_2]}{1 + K_{H,A}[A] + K_{H,B}[B]}\right]C_{cat}{}^p$$

$$\frac{d[B]}{dt} = r_{h,B} + r_{H,B}C_{cat}{}^p \quad (7)$$

$$= k_{h,1}[A][H_2O_2] - k_{h,3}[B][H_2O_2] + \left[\frac{k_{H,1}K_{H,A}[A][H_2O_2]}{1 + K_{H,A}[A] + K_{H,B}[B]} - \frac{k_{H,2}K_{H,B}[B][H_2O_2]}{1 + K_{H,A}[A] + K_{H,B}[B]}\right]C_{cat}{}^p$$

where the initial conditions are $[A] = [A]_0$ and $[B] = 0$ at $t = 0$. Note that, in each part of eqs 7, the first term on the right-hand side gives the homogeneous contribution to the rate, and the second term gives the heterogeneous contribution.

Parameter Identification. The parameters of the proposed apparent kinetics models were determined according to two steps as mentioned earlier. In the first step, the homogeneous kinetics rate constants, $k_{h,1}$, $k_{h,2}$, and $k_{h,3}$, were determined using the homogeneous experimental data, which were obtained at three different temperatures and three different phenol initial concentrations in the absence of solid catalysts. In the second step, the parameters, including heterogeneous reaction rate constants $k_{H,1}$ and $k_{H,2}$, adsorption−desorption equilibrium constants $K_{H,A}$ and $K_{H,B}$, and the exponent term for catalyst loading p, were identified according to the heterogeneous experimental data and the rate constants obtained in the first step. As discussed earlier, the heterogeneous experimental data were measured at four different temperatures, four different phenol initial concentrations, four different H_2O_2 inlet concentrations, and three different catalyst loading concentrations.

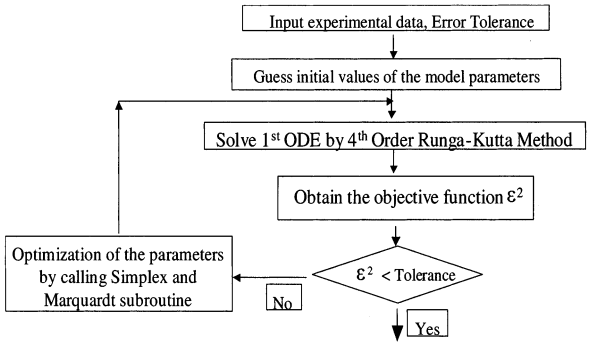

Figure 11. Schematic diagram for model parameter identification.

A schematic diagram for the parameter determinations is presented in Figure 11. First, the kinetic parameters for phenol oxidation by oxygen were taken from the literature to act as the initial guess for the current model parameters, because few kinetic parameters were available for the phenol oxidation by H_2O_2. Then, the fourth-order Runga−Kutta numerical method[27] was utilized to solve the ordinary differential equation systems, i.e., eqs 3 for noncatalytic reaction and eqs 7 for catalytic reaction, to simulate the concentration evolution of lumps A and B. The least-squares optimization was set as the objective function (eq 8) to evaluate the parameters for both the noncatalytic reaction model (eqs 3) and the catalytic reaction model (eqs 7)

$$\epsilon^2 = \sum_{i=1}^{n}\left[\left(\frac{[A]_{sim} - [A]_{exp}}{[A]_{exp}}\right)^2 + \left(\frac{[B]_{sim} - [B]_{exp}}{[B]_{exp}}\right)^2\right] \quad (8)$$

where the subscripts exp and sim stand for the experimental and simulated values, respectively. A Fortran program was developed in which the Simplex−Marquardt algorithm[28] was used to minimize the objective function (eq 8) via nonlinear least-squares fitting of the experimental data. Convergence was considered to be achieved when the model predicted values of lump concentrations were adequately matched with the corresponding experimental data for all catalyst loadings, temperatures, initial phenol concentrations, and inlet H_2O_2 concentrations covered in the current study.

The fitted reaction rate parameters for the homogeneous (noncatalytic) and heterogeneous (catalytic) reactions are summarized in Table 1.

Model Evaluation and Discussion. A kinetic model is valid only if it truly reflects experimental results for given conditions. For the homogeneous reaction, typical results of the model predictions and experimental data are shown in Figure 12, where the effect of different temperatures on the noncatalytic phenol removal rate is tested. Figure 13 is a parity plot that compares the experimental observations with the results calculated from eqs 3. No trend can be noticed, and most of the

Table 1. Rate Parameters for the Homogeneous and Heterogeneous Reactions

homogeneous reaction	heterogeneous reaction
$k_{h,1} = 0.028e^{-13\,157/RT}$	$k_{H,1} = 207.02e^{-6447.4/RT}$
$k_{h,2} = 2178.91e^{-47\,683/RT}$	$k_{H,2} = 3.78e^{-8437.1/RT}$
$k_{h,3} = 736.52e^{-44\,596/RT}$	$K_{H,A} = 0.0024e^{-6709.7/RT}$
	$K_{H,B} = 12.01e^{-19\,791/RT}$
	$p = 0.798$

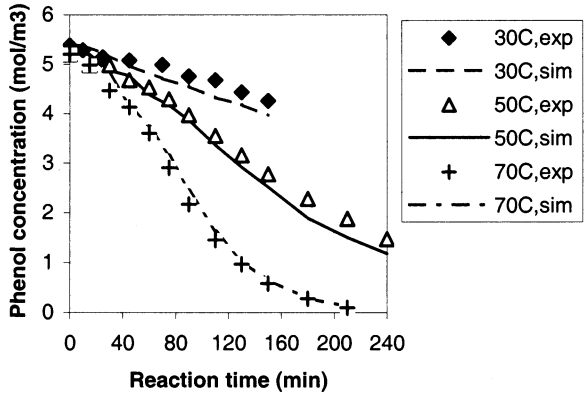

Figure 12. Measured and predicted time profiles for phenol removal in the homogeneous reaction at different temperature (500 ppm phenol, 0.3 M H_2O_2).

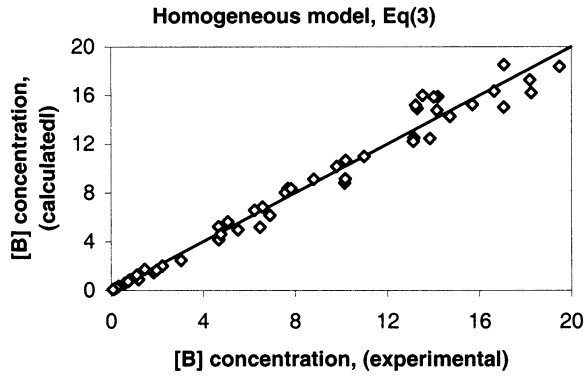

Figure 13. Parity plot for lump B concentration (mol/m^3) in the homogeneous reaction.

relative residuals are bounded within ±15%, with the average absolute relative error (AARE) equal to 8.1%. Thus, reasonably good fits of the desired reactant and product compositions were achieved for the homogeneous reaction.

The prediction results based on the catalytic reaction model agree well with the experimental measurements of lump A and B obtained at temperatures from 30 to 90 °C, as shown in Figure 14. Figure 15 presents the calculated concentration values for the intermediate products obtained with this model, where most of the relative residual values are bounded within ±20%. The average absolute relative error (AARE) is 9.2%. Consequently, the homogeneous−heterogeneous approach as a tool in the kinetics analysis for complex reaction systems demonstrates its feasibility and usefulness.

Compared to the noncatalytic route, the catalytic route reduces the activation energies or increases preexponential factors. Catalysts can expedite chemical reaction processes by lowering the activation energy barrier or enhancing the chances of reactant collision. The activation energies for the degradation of phenol into intermediate products and the mineralization of the intermediate products are 6.447 and 8.437 kJ/mol in

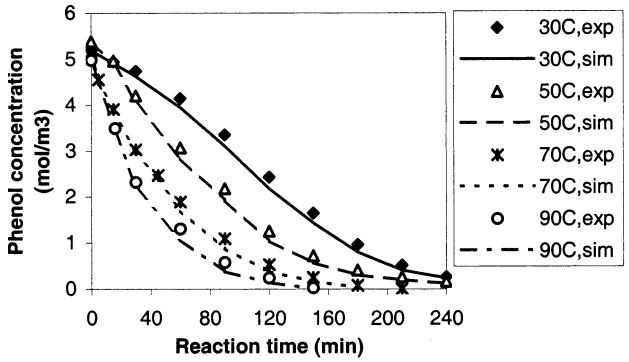

Figure 14. Measured and predicted time profiles of phenol removal at different temperatures (6.6 g/L catalyst, 500 ppm phenol, 0.3 M H_2O_2).

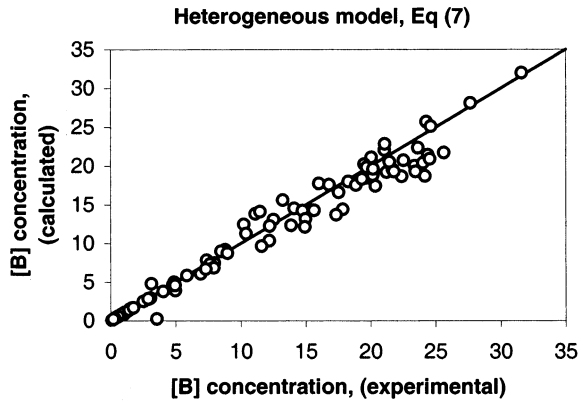

Figure 15. Parity plot for lump B concentration (mol/m^3) in the heterogeneous reaction.

heterogeneous reaction, and the counterparts in homogeneous reaction are 13.157 and 44.596 kJ/mol, respectively. In addition, the high value of the activation energy for the mineralization of intermediate products without catalyst demonstrates the recalcitrance of the intermediates.

Because of the role played by the catalyst in the generation of free radicals that can propagate in the liquid phase, the models based on separate kinetics for homogeneous and heterogeneous contributions do not yield a good prediction of the experimental results without accounting for the catalyst loading. The heterogeneous reaction model proposed here takes into account a potential term for the catalyst concentration, whose exponent was determined to be 0.798 for both the phenol removal and the variation of the intermediate organics.

To our knowledge, this is the first study that describes unambiguously the homogeneous and heterogeneous approach to the issue of phenol oxidation with hydrogen peroxide. No literature record is available for the global kinetics expression and reaction rate constants of the phenol oxidation reaction. Thus, more detailed kinetics studies on the interaction between heterogeneous and significant homogeneous reactions should give rise to new understanding concerning CWO technology.

Conclusion

The catalytic wet oxidation of aqueous phenol using hydrogen peroxide occurred both on the catalyst surface and in the liquid bulk phase. The catalyst showed an optimal performance at a pH of about 4.0. The reaction

is initiated by a radical mechanism that is promoted by initial pH control. The phenol conversion curves showed that increasing the temperature, catalyst loading, and H_2O_2 concentration improved the rate of phenol removal, whereas self-inhibition of phenol was demonstrated as the higher phenol initial condition led to a lower phenol degradation rate.

Wet oxidation of phenol with hydrogen peroxide over mixed Al−Fe pillared clay catalyst has been demonstrated to be a powerful method for the removal of low-concentration aqueous phenol under very mild conditions (1 atm, <90 °C) without appreciable loss of catalyst activity.

The apparent kinetics of catalytic wet peroxide oxidation was treated using a homogeneous−heterogeneous model, which described well the time dependence of the concentrations of phenol and intermediate products. This model captures the reaction network scheme, reflecting the homogeneous noncatalytic reaction oxidation based on a set of second-order reactions and the heterogeneous catalytic reaction pathway in the framework of a LHHW scheme.

Considering the cost and corrosion issues of hydrogen peroxide reagent, our future work will focus on the feasibility of efficiently removing phenol by only air or by a combination of air and less H_2O_2.

Acknowledgment

The authors thank professor N. Papayannakos of the National Technical University of Athens (NTUA), Athens, Greece, for the kind supply of the mixed Al−Fe pillared clay catalyst. The financial support for the Chemical Reaction Engineering Laboratory (CREL) of Washington University, St. Louis, MO, is gratefully acknowledged.

Notation

AARE = average absolute relative error, AARE = $\sum_{i=1}^{N}|(y_{sim,i} - y_{exp,i})/y_{exp,i}|/N$
[A] = phenol concentration, (mol of C)/(m^3 of solution)
[B] = concentration of dissolved intermediate organic lump, (mol of C)/(m^3 of solution)
[C] = carbon concentration of end-product lump, (mol of C)/(m^3 of solution)
[H_2O_2] = concentration of H_2O_2, mol/(m^3 of solution)
C_{cat} = catalyst concentration, (kg of catalyst)/(m^3 of solution)
K = adsorption equilibrium constant, m^3/mol
k_H = heterogeneous reaction rate constant, [m^3/(kg of catalyst)]^p/min
k_h = homogeneous reaction rate constant, m^3/(mol min)
p = potential order for the catalyst loading influence in heterogeneous model
r_h = reaction rate due to homogeneous contribution, (mol of C)/[(m^3 of solution) min]
r_H = reaction rate due to heterogeneous contribution, (mol of C) (m^3 of solution)$^{p-1}$/(kg^p min)
t = reaction time, min
T = temperature, K or °C
TOC = total organic carbon, (mol of C)/(m^3 of solution)
u = inlet flow rate of H_2O_2, mL/min
V = volume of the aqueous solution, mL

Subscripts and Superscripts

* = free site, adsorbed
A = phenol lump
B = dissolved organic intermediate lump
exp = experimental data
h = homogeneous reaction
H = heterogeneous reaction
sim = simulation data

Literature Cited

(1) Yurii, I. M. M.; Moshe, S. Catalytic Abatement of Water Pollutants. *Ind. Eng. Chem. Res.* **1998**, *37*, 309.

(2) Moore, J. W.; Ramamoorthy, S. *Organic Chemicals in Natural Waters*; Springer-Verlag: New York, 1984.

(3) Mann, M. D.; Wilson, W. G.; Hendrikson, J. G. Gasifier Wastewater Treatment: Phase I Cooling Tower Assessment. *Environ. Prog.* **1985**, *4* (1), 33.

(4) Aurora, S.; Pedro, Y.; Beatriz, D.; Felix, G. O. Catalytic Wet Oxidation of Phenol: Kinetics of the Mineralization Rate. *Ind. Eng. Chem. Res.* **2001**, *40*, 2773.

(5) Brock, T. D.; Madigan, M. T. *Biology of Microorganisms*; Prentice Hall: Englewood Cliffs, NJ, 1988.

(6) Larachi, F.; Iliuta, I.; Belkacemi, K. Catalytic Wet Air Oxidation with a Deactivating Catalyst Analysis of Fixed and Sparged Three-Phase Reactors. *Catal. Today* **2001**, *64*, 309.

(7) Dojlido, R.; Best, G. A. *Chemistry of Waters and Water Pollution*; Ellis Horwoood: New York, 1993.

(8) Autenrieth, R. L.; Bonner, J. S.; Akgerman, A.; Okaygun, M.; Mccreary, E. M. Biodegradation of Phenolic Wastes. *J. Hazard. Mater.* **1991**, 28.

(9) Imamura, S. Reviews: Catalytic and Noncatalytic Wet Oxidation. *Ind. Eng. Chem. Res.* **1999**, *38*, 1743.

(10) Bond, G. C. *Heterogeneous Catalysis: Principles and Applications*; Oxford University Press: Oxford, U.K., 1974.

(11) Keckler, K. P.; Brandenburg, B. L.; Momont, J. A.; Lehman, R. W. Treatment of Wastewater from Acrylonitrile Manufacturing Plant. *Chem. Abstr.* **1993**, *118*, 197432.

(12) Luck, F. A Review of Industrial Catalytic Wet Air Oxidation Processes. *Catal. Today* **1996**, *27*, 195.

(13) Hamoudi, S.; Larachi, F.; Graciela, C.; Myrian, C. Wet Oxidation of Phenol Catalyzed by Unpromoted and Platinum-Promoted Manganese/Cerium Oxide. *Ind. Eng. Chem. Res.* **1998**, *37*, 3561.

(14) Hamoudi, S.; Belkacemi, K.; Larachi, F. Catalytic Oxidation of Aqueous Phenolic Solutions: Catalyst Deactivation and Kinetics. *Chem. Eng. Sci.* **1999**, *54*, 3569.

(15) Moser, W. R. *Advanced Catalysts and Nanostructured Materials*; Academic Press: San Diego, CA, 1996.

(16) Barrault, J.; Abdellaoui, M.; Bouchoule, C.; Majeste, A.; Tatibouet, J. M.; Louloudi, A.; Papayannakos, N.; Gangas, N. H. Catalytic Wet Peroxide Oxidation over Mixed (Al−Fe) Pillared Clays. *Appl. Catal. B: Environ.* **2000**, *27*, 225.

(17) Pintar, A.; Levec, J. Catalytic Liquid-Phase Oxidation of Phenol Aqueous Solutions: A Kinetic Investigation. *Ind. Eng. Chem. Res.* **1994**, *33*, 3070.

(18) Shende, R. V.; Levec, J. Wet Oxidation Kinetics of Refractory Low Molecular Mass Carboxylic Acids. *Ind. Eng. Chem. Res.* **1999**, *38*, 3830.

(19) Fortuny, A.; Ferrer, C.; Bengoa, C.; Font, J.; Fabregat, A. Catalytic Removal of Phenol from Aqueous Phase Using Oxygen or Air as Oxidant. *Catal. Today* **1995**, *24*, 79.

(20) Ding, Z. Y.; Frisch, M. A.; Li, L.; Gloyna, E. F. Catalytic Oxidation in Supercritical Water. *Ind. Eng. Chem. Res.* **1996**, *35*, 3257.

(21) Sadana, A.; Katzer, J. R. Involvement of Free Radicals in the Aqueous-Phase Catalytic Oxidation of Phenol over Copper Oxide. *J. Catal.* **1974**, *35*, 140.

(22) Bishop, D. F.; Stern, G.; Fleischman, M.; Marshall, L. S. Hydrogen Peroxide Catalytic Oxidation of Refractory Organics in Municipal Wastewater. *Ind. Eng. Chem. Process Des. Dev.* **1968**, *7*, 110.

(23) Pintar, A.; Levec, J. Catalytic Oxidation of Organics in Aqueous Solutions: Kinetics of Phenol Oxidation. *J. Catal.* **1992**, *135*, 345.

(24) Gangas, N. H.; Papayannakos, N. G. *Final Report of Feasibility Award FA-1010-91*; Contract Number BRE2-063; 1993; Sections III.4−III.6.

(25) Hamoudi, S.; Belkacemi, K.; Sayari, A.; Larachi, F. Catalytic Oxidation of 4-Chloroguaiacol Reaction Kinetics and Catalyst Studies. *Chem. Eng. Sci.* **2001**, *56*, 1275.

(26) Li, L.; Chen, P.; Gloyna, E. Generalized Kinetic Model for Wet Oxidation of Organic Compounds. *AIChE J.* **1991**, *37*, 1687.

(27) Press, H. W.; Teukolsly, S. A.; Vetterling, W. T.; Flannery, B. P. *Numerical Recipes, The Art of Scientific Computing*; Cambridge University Press: Cambridge, U.K., 1992.

(28) Duggleby, R. G. Regression Analysis of Nonlinear Arrhenius Plots: An Empirical Model and a Computer Program. *Comput. Biol. Med.* **1984**, *14*, 447.

Received for review May 6, 2002
Revised manuscript received October 18, 2002
Accepted October 21, 2002

IE020344T